The Influence of Electron Radiation on $ZnS\text{-}SiO_2$ Films

Atsuko Kojima, Eriko Mizoguchi, Midori Takano

Characterization Technology Group, Matsushita Technoresearch, Inc.
3-1-1, Yagumo-Nakamachi, Moriguchi, Osaka, 570-8501 JAPAN

(Received October 12 1998; accepted January 13 1999)

Electron-beam-induced damage to $ZnS\text{-}SiO_2$ protective layers has been found to result in S desorption and enhanced sputter etching. In this report, the influence of current density on electron-beam-induced damage to $ZnS\text{-}SiO_2$ films is presented. Both S and Zn Auger peak intensities decrease with increased beam irradiation time, whereas the Si and O peak heights increase with increasing irradiation time. The electron irradiation also changes the zinc sulfide to zinc metal, and the resulting surface is rapidly oxidized by air exposure. The surface roughness of the samples is also increased by the electron beam.

1. Introduction

Phase-change optical disks are composed of $ZnS\text{-}SiO_2$ / Te-Ge-Sb / $ZnS\text{-}SiO_2$ layered structures. It is important to estimate inter-diffusion at the interface of the $ZnS\text{-}SiO_2$ protective layer and the Te-Ge-Sb recording layer accurately, as it is closely related to the reliability of the optical disk. The combination of Auger electron spectroscopy (AES) and simultaneous ion-beam sputter etching is widely used to obtain compositional depth profiles of these disks. Because of the electron and/or ion beam interactions with these insulating samples, artifacts in the analysis are common [1][2]. We have previously reported electron-beam-induced damage of the $ZnS\text{-}SiO_2$ protective layers in these systems. The desorption of S and diffusion of Zn induced by electron irradiation results in increased surface roughness and degradation in AES depth resolution [3].

In this paper, we describe the changes in the AES peak intensities and shapes of the $ZnS\text{-}SiO_2$ layer during electron irradiation. We also report the XPS and AFM studies of the electron-irradiated surface and discuss the influence of an electron beam on $ZnS\text{-}SiO_2$ films.

2. Experimental

The samples used for this study were 95 nm-thick-$ZnS\text{-}SiO_2$ films deposited on quartz substrates.

In order to examine both the surface morphology and surface chemistry of the films after electron irradiation, the samples were studied with XPS and AFM. The irradiation was performed with a JEOL JAMP-10s, using a primary electron beam energy of 3 keV and a beam current of 0.5μA. The electron-irradiated area was 1.2mm x 1.2mm, yielding a current density of about $0.4\mu A/mm^2$.

AES measurements were performed with a PHI 670, using a primary electron beam energy of 3 keV with a beam current of 10nA. The current densities were set to about $3\mu A/mm^2$, $0.3\mu A/mm^2$, and $0.03\mu A/mm^2$ by changing the electron beam raster area. Ar^+ ion sputtering was done with an ion beam energy of 3 keV to remove surface contamination. The electron gun and the ion gun were mounted 70° and 30° relative to the sample surface normal, respectively. The Auger lines measured were Si LVV, S LVV, O KLL and Zn LMM. The Auger signals were detected in the direct mode with pulse counting. Peak-to-peak Auger intensities were plotted after a 5-point differentiation.

XPS measurements were performed with a PHI 5400MC, using MgKα x-rays. XPS photolines measured were Si 2p, S 2p, O1s, Zn 2p and the Zn LMM Auger line.

AFM measurements were performed in the tapping mode with a Topo Metrix TMX-2000 Atom Tracer.

3. Results and discussions

3.1 *In situ* study of the AES peak heights and shapes during electron irradiation

Figure 1 shows the electron irradiation time dependence of the AES peak heights with current densities of 3, 0.3, and $0.03\mu A/mm^2$. Both S and Zn peak intensities decrease with increased beam irradiation time, whereas Si and O peak heights increase with increasing

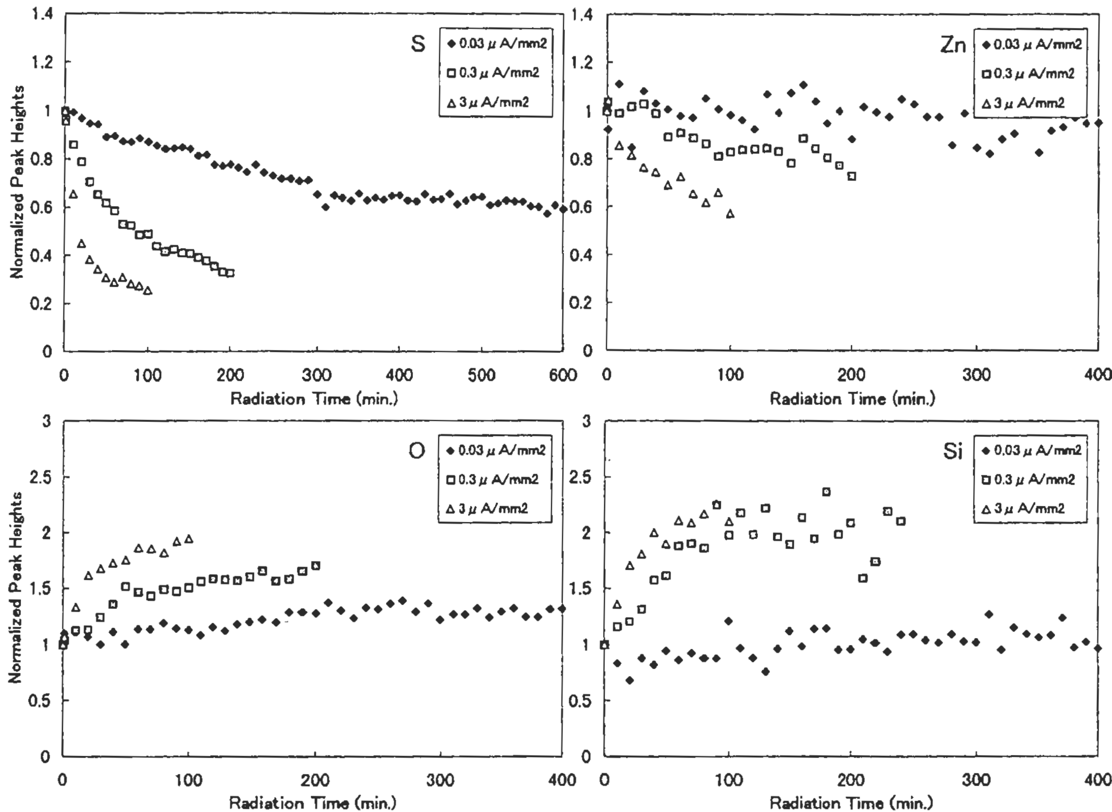

Figure 1 The electron irradiation time dependence of intensity ratio on ZnS-SiO_2 film. The peak heights are normalized at the value of 0min.

irradiation time. The current density dependence of the converged peak heights of these elements is shown in Figure 2. If these changes were caused by electron beam heating, these peak heights would be proportional to the current densities. However, they change steeply under the lower current densities.

We found that S is desorbed at 300 ℃ by previous Thermal Desorption Mass Spectrometry (TDMS) study, while no Zn desorption was detected in the TDMS pyrogram[3]. Therefore we suppose that the electron beam heating is not only the reason of these peak height change.

The AES spectra are shown in Figure 3. The peak shapes do not appear to be very different after 100 min of irradiation. After irradiation, there is a consistent shift in the energies of the Auger peaks by about -3 eV. We attribute this to positive charging of the irradiated surface. Sample charging may cause Zn peak height reduction. However, this phenomenon was not reproduced on an electrically biased sample.

3.2 *Ex situ* XPS and AFM study of the electron-irradiated surface

Figure 4 shows the XPS spectra of the ZnS-SiO_2 surface before and after electron

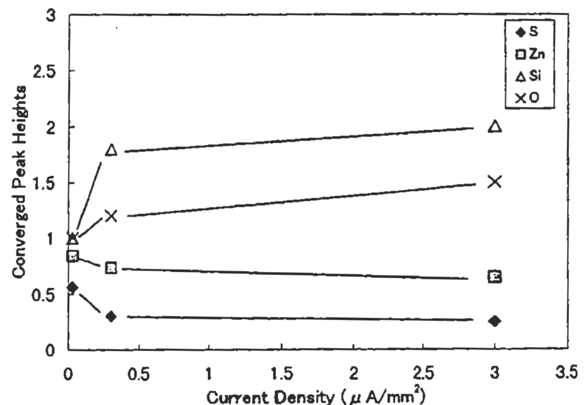

Figure 2. Electron beam current density dependence of converged peak heights.

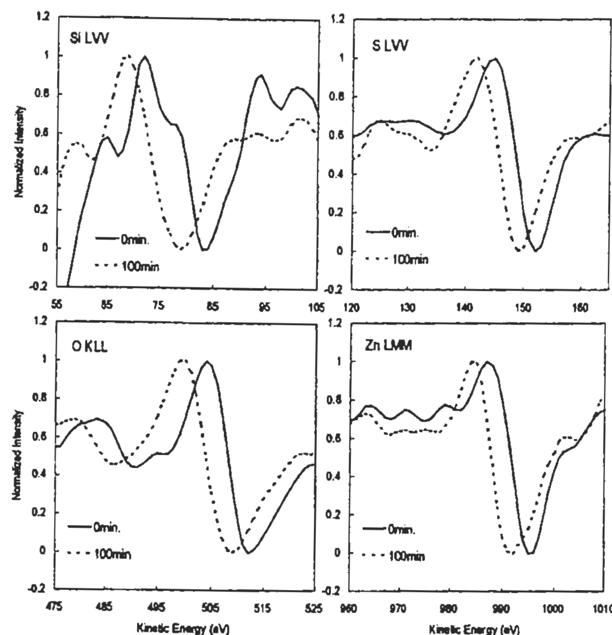

Figure 3. The AES spectra of .Si LVV, S LVV, O KLL, Zn LMM at 0minute and 100minutes.irradiation.

irradiation. The data shows that Zn and O increase and Si and S decrease on the surface of the sample after irradiation. Table 1 shows the photoelectron and Auger electron peak positions, before and after irradiation, compared with some standard materials[4]-[9]. The Zn LMM and O 1s peak positions suggest that the zinc is bonded mainly to S before irradiation, and to O after electron irradiation. The S and Si peak energies are not affected by the sample treatment.

The AES *in situ* analysis shows that S/Zn peak height ratio decreases during irradiation. We believe that zinc sulfide changes to zinc metal in the vacuum chamber and that the sample surface is then oxidized by when sample was exposed to the air before the XPS measurements.

Figure 5 shows an AFM of the ZnS-SiO_2 surface before and after electron irradiation. Electron irradiation increased the surface roughness. The standard roughness (Ra) is 0.2nm before irradiation, while it is 0.8nm after irradiation. About 70 pits were

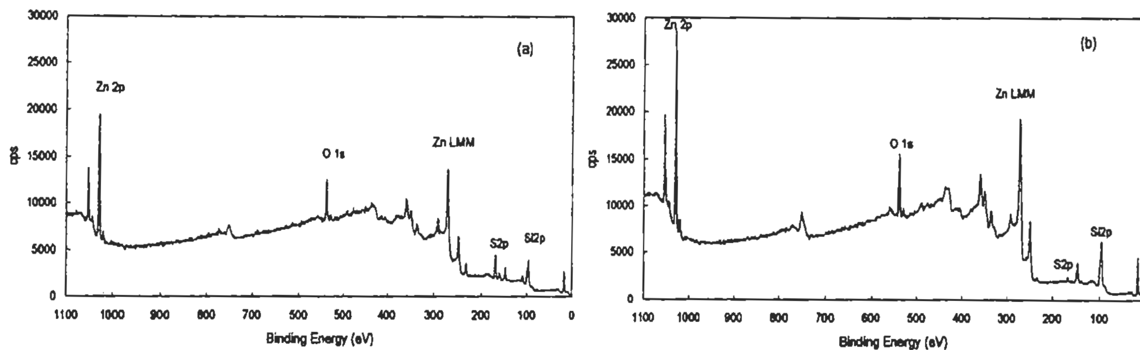

Figure 4. The XPS spectra of ZnS-SiO_2 surface (a) before and (b) after electron irradiation

Table 1 Photoelectron and Auger Electron Spectrum line (eV)

Sample	S2p	Si2p	O1s	Zn LMM	Zn2p3
before irradiation	161.8	102.0	530.6 531.6	988.7	1021.8
after irradiation	161.8	102.0	530.4 532.0	988.1	1021.8
Zn				992.3	1021.6
ZnS	161.5			989.9	1021.8
ZnO			530.2	988.7	1021.6
$Zn_4Si_2O_7(OH)_2 \cdot 2H_2O$		101.8		987.5	1021.8

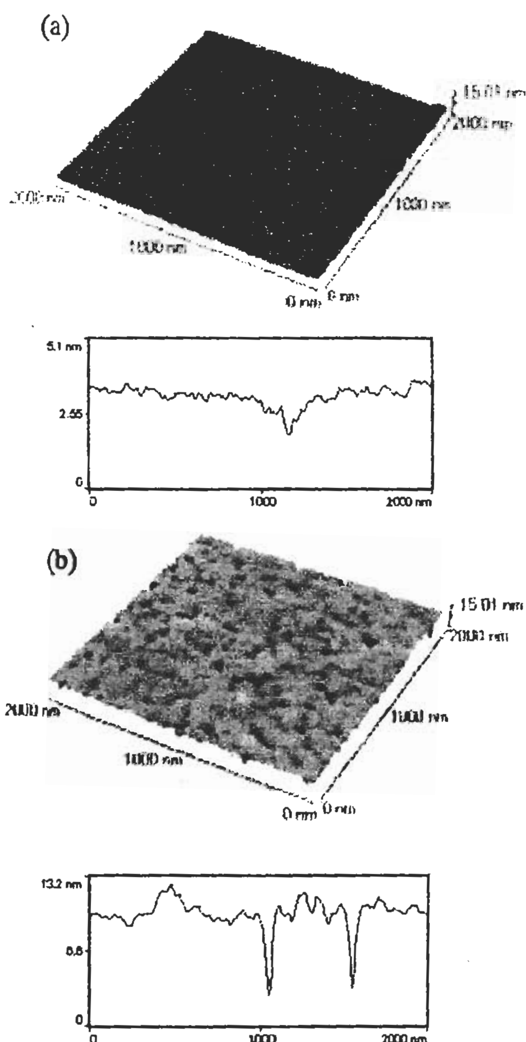

Figure 5. The AFM bird view and line profile of ZnS-SiO2 surface (a) before (b) after electron irradiation

observed on the irradiated surface, with diameters of about 50nm. If we assume that these pitted areas do not contribute to total electron emissions, then the expected reduction in emission intensity would be to about 95% of that of the unpitted surface. However, the in situ Zn intensity decreased by about 20%. Surface roughness was therefore not the main reason for the drop in Zn peak heights of these samples.

Figure 6 shows an AES depth profile of the sample studied with XPS. A 3nm-thick sulfur-deficient layer was observed. Zn piled up under the sulfur-deficient layer. These result suggests that S desorption contributes to the surface roughness of the irradiated samples and that Zn migrate away from the surface.

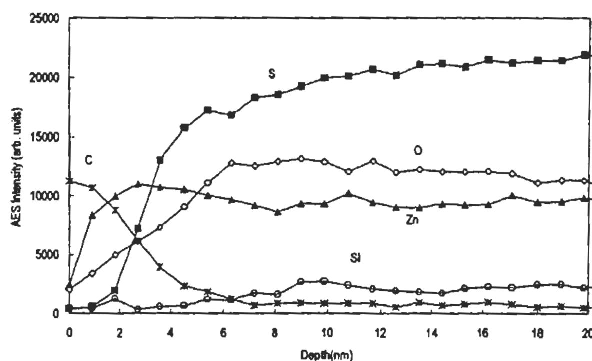

Figure 6. The AES depth profile of the sample studied with XPS and AFM

4. Conclusions

We studied the electron-irradiated surface of $ZnS-SiO_2$ films. We found that electron-beam-irradiation induced surface S desorption and Zn migration. We also determined that the 3 nm thick S-deficient layer is rapidly oxidized by air exposure, that surface roughness is enhanced by the electron-beam-induced S desorption, and that the final S AES peak height depends on the current density of the beam applied.

References

[1] J. Ahn, C.R. Perleberg, D.L. Wilcox, J.W. Coburn and H.F. Winters, J. Appl. Phys. 46, 4581 (1975).

[2] L.F. Vassamillet and V.E. Caldwell, J. Appl. Phys. 40, 1637 (1969).

[3] A. Kojima, T. Matsunaga and N. Yamada, J. Surf. Anal. Vol.4 No.1, 42 (1998).

[4] C.D. Wagner, W.M. Riggs, L.E. Davis, J.F. Moulder, G.E. Mullenberg, Handbook of X-ray Photoelectron Spectroscopy, Perkin-Elmer Corporation, Physical Electronics Division, Eden Prairie, MN55344 (1979).

[5] S.W. Gaarenstroom, N. Winograd, J. Chem. Phys. 67, 3500 (1977).

[6] B.R. Strohmeier, D.M.Hercules, J.Catal.86, 266 (1984).

[7] G. Schoen, Acta Chem.Scand. 27, 2623 (1973)

[8] G. Schoen, J. Electron Spectrosc. Relat. Phenom. 2, 75 (1973).

[9] C.D. Wagner, D.E. Passoja, H.F. Hillery, T.G. Kinisky, H.A. Six, W.T. Jansen, J.A. Tylor, J.Vac.Sci.Tecnol. 21, 933 (1982).